Digital Holography Based on Aperture Engineering

by Joseph Rosen, Vijayakumar Anand, and Nathaniel Hai

doi: http://dx.doi.org/10.1117/3.2670001
PDF ISBN: 9781510662445

Published by

SPIE Press
P.O. Box 10
Bellingham, Washington 98227-0010 USA
Phone: +1 360.676.3290
Fax: +1 360.647.1445
Email: Books@spie.org
Web: http://spie.org

Spotlight vol. SL66
Last updated: 5 July 2023

SPIE.

Table of Contents

1 Introduction

Innovations and inventions can sometimes be nothing more than a new and unexpected combination of well known and unrelated ideas. Digital holography based on phase aperture engineering is such a case of a mosaic of general concepts from different fields of interest. Digital holography was born with Goodman and Lawrence's pioneering study,[1] and the intensive research on this topic in the last five decades has been reviewed lately in a Roadmap article.[2] Phase aperture digital holography (PADH), studied during the last two decades under different names, is a subfield of the general digital holography and is the main topic of this Spotlight review. In general, in PADH, the light from the observed scene is modulated by at least one engineered phase element used as the system's aperture.[3] As we show in the following, methods from unrelated fields, such as adaptive optics, pattern recognition, signal processing, optical and computational imaging, beam shaping, x-ray imaging, and optical interferometry, are fused and adapted for diverse imaging applications by various PADH configurations. The main goal of this fusion of methods is to improve the performance of the hologram recorders and to enable new applications using this technology. The transition of ideas from unconnected areas can be a good lesson for everyone who wants to improve the existing technology. Sometimes the best solution in one field belongs to a different area of interest, and the only needed creativity is the proper adaptation from one field to the other. As discussed in the next paragraph, such a transition also happened in the first decade of the present millennium. At that time, researchers looked for a nonscanning three-dimensional (3D) imaging technique for incoherently illuminated objects and found a new method of incoherent digital holography. Before we continue, it should be emphasized that the term "incoherent light" throughout this review refers to quasimonochromatic spatially incoherent light.

In recent years, there has been an increased interest in incoherent digital holography techniques for several reasons, such as the requirement of imaging fluorescent specimens,[4] the desire to image 3D scenes from a single point of view[5] with minimal camera shots,[6] and the possibility of using new reliable phase-only spatial light modulators (SLMs).[7] One such digital holography technique is Fresnel incoherent correlation holography (FINCH), as published in 2007 and later.[8,9] FINCH was proposed as an alternative to the scanning-based holography methods, such as optical scanning holography[4,5,10] and multiple view projection holography.[6,11] In both scanning techniques, the recorded hologram is the sum along the z axis of two-dimensional (2D) cross-correlations between the objects and quadratic phase functions. At that time, the challenge was to perform these cross-correlations without scanning or movement. The inspiration for FINCH came from optical motionless incoherent correlators[12] with the appropriate adaptation to holographic systems using the self-interference principle[13] and phase-shifting interferometry.[14] By self-interference principle, we mean that the

the same NA. The correlation length depends on the average size of the speckle, which is $\sim 1.22\lambda z/D$, where z is the distance between the observed object and the system's aperture.[113,114] Consequently, the speckle size variation follows the same trend as lens-based imaging systems, resulting in the same axial resolution. For the above simulation conditions, the axial resolution was compared between FINCH and COACH cases. The variation in the axial intensity is given as $O_R(z) = H_{\mathrm{PSH}}(z=0) \otimes H_{\mathrm{PSH}}(z)$. The distance object-aperture is varied from 20 to 80 cm, and the plots of $I_A(x=0, y=0, z)$ for COACH ($\sigma = 0.2$), FINCH, and lens-based imaging are compared in Fig. 8. As expected, the axial resolution of COACH is similar to that of lens-based imaging and better than that of FINCH.

An object consisting of two planes was constructed by mounting two identical smiley objects with different lateral locations and axial separation of 5 cm. The reconstruction results using lens-based imaging, FINCH, and COACH are shown in Figs. 9(a)–9(c), respectively. As expected, in FINCH, the background object information is prominent, indicating its low axial resolution. In COACH and lens-based imaging, the background object information is diminished. The reconstruction in COACH was carried out using a phase-only filter. The noise level in COACH is higher than in FINCH and lens-based imaging.

2.3 Fourier incoherent single-channel holography

Fourier incoherent single-channel holography, abbreviated as FISCH, is a method for recording digital Fourier holograms with incoherent illumination.[106,107] FISCH was proposed in 2012 to reduce the number of required camera shots needed for

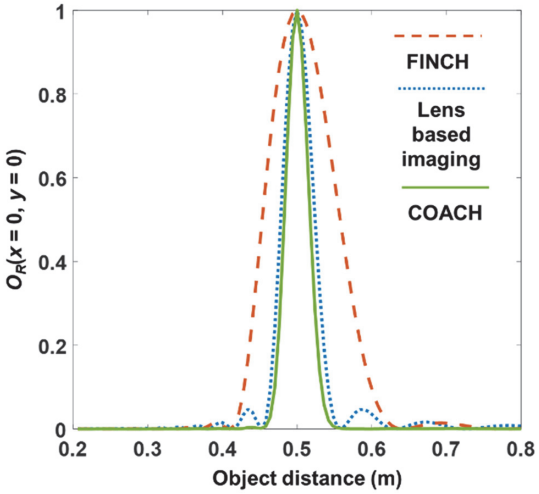

Figure 8 Plots of the normalized axial correlation value O_R (defined in the text for COACH and FINCH) and intensity value (lens-based imaging) at the origin for different object distances.

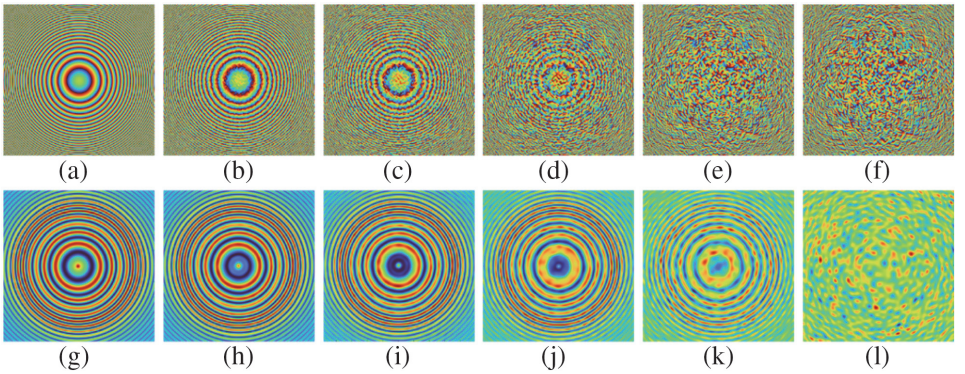

Figure 13 (top) Phase images displayed on a SLM for (a) $\alpha = 0$, (b) $\alpha = 0.2$, (c) $\alpha = 0.4$, (d) $\alpha = 0.6$, (e) $\alpha = 0.8$, and (f) $\alpha = 1$. (bottom) Images of PSHs for (g) $\alpha = 0$, (h) $\alpha = 0.2$, (i) $\alpha = 0.4$, (j) $\alpha = 0.6$, (k) $\alpha = 0.8$, and (l) $\alpha = 1$.

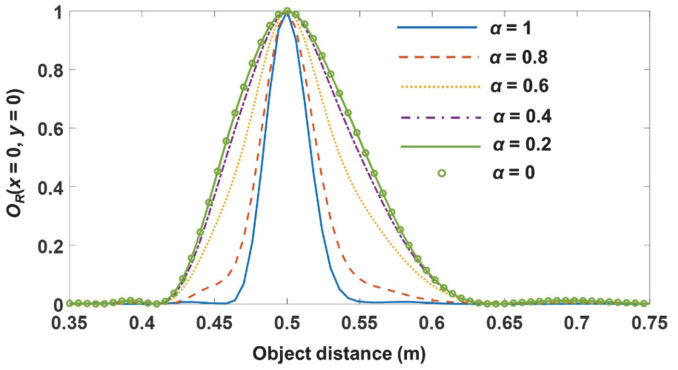

Figure 14 Plots of the normalized axial correlation value O_R for $\alpha = 0$, 0.2, 0.4, 0.6, 0.8, and 1 at the origin for different object distances.

The axial intensity variation is studied and compared for $\alpha = 0$ to 1. The plots of the axial correlation intensity $O_R(z, x = 0, y = 0)$ for an object-aperture distance variation of 20 to 80 cm for $\alpha = 0$ to 1 are shown in Fig. 14. It seems that the axial resolution is improved with the increase in α. Next, we study the imaging of two planar objects consisting of the same smiley objects axially separated by a distance of 5 cm and laterally separated. The reconstruction results using the hybrid system for $\alpha = 0$ to 1 are shown in Figs. 15(a)–15(f), respectively. Apparently, the noise level increases with an increase in α, and the axial resolution is improved with an increase in α.

2.5 Synthetic apertures using aperture engineering

The development of optical incoherent SA began with the seminal work of Michelson and Pease, published in 1921.[120] Since then, all astronomical

corresponding images of direct imaging with a setup of a single lens and similar NAs. The stitched holograms after the superposition are shown in Fig. 17(b). Figure 17(c) presents the reconstructed images for OCTISAI with various area sizes of the SA holograms. Figures 17(c_1) and 17(c_2) are produced using the central eight, horizontally [Fig. 17(c_1)] and vertically, [Fig. 17(c_2)] stitched partial holograms, respectively. Figures 17(c_3)–17(c_6) show the reconstruction results with 2 × 2, 4 × 4, 6 × 6 central subholograms and all 64 subholograms. The resolution enhancement by raising the number of stitched partial holograms is demonstrated. Comparing Fig. 17(c_6) with Figs. 17(a_1) and 17(a_3), one can conclude that OCTISAI's images have higher resolution than the images taken with a limited aperture in both techniques of COACH and direct imaging.

3 Interferenceless Incoherent Digital Holography

3.1 Interferenceless COACH

I-COACH[25] was developed during the investigation of COACH.[21] While it may appear that the difference between COACH and I-COACH is only in the reference wave that exists in COACH and not in I-COACH, the imaging principles differ. In COACH, the light from every object point is divided into two: one part is modulated by a quasirandom phase mask and interfered with the unmodulated part as in any incoherent digital holography system. So, COACH required multiple camera shots with different phase shifts to remove the twin image and bias terms during reconstruction. Unlike FINCH, the reconstruction of COACH is carried out using cross-correlation with the PSH. In I-COACH, as shown in Fig. 18, the light from every object point is scattered by a quasirandom phase mask, so the recorded intensity distribution for an object is the summation of the shifted 3D PSHs. If the 3D PSH is known, then by correlating it with the recorded object intensity distribution, the 3D image of the object can be reconstructed. Therefore, a static aperture is sufficient in I-COACH, and multiple camera shots with phase shifts are not needed as in COACH or FINCH. The first version of I-COACH[25] still involved multiple

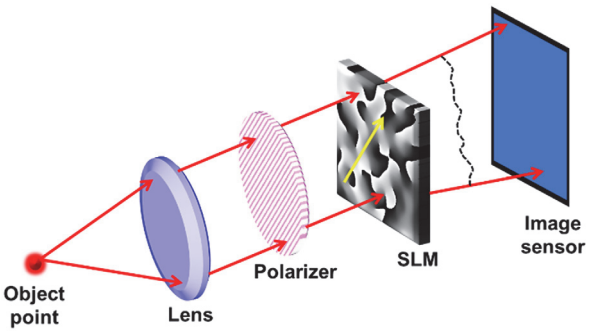

Figure 18 Optical configuration of I-COACH. The yellow arrow indicates the active axis of the SLM.

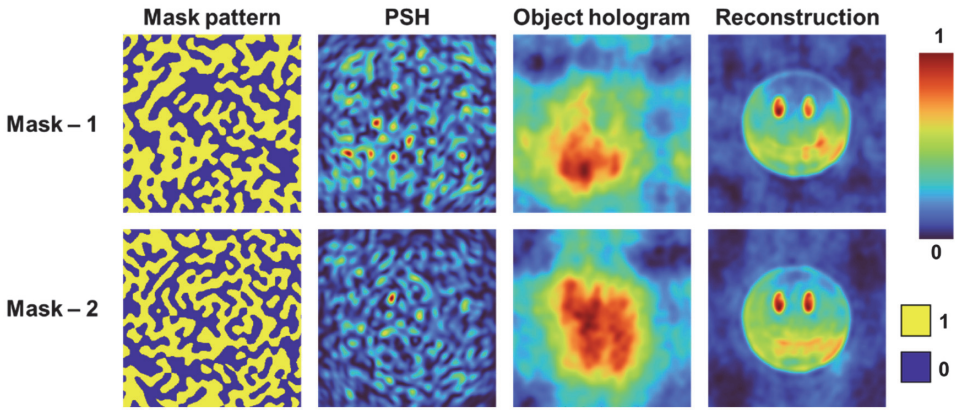

Figure 23 Mask patterns with space constraint and space and phase constraints, PSHs, OHs, and reconstruction results.

reciprocity was used to synthesize PSHs for different wavelengths rather than a PSH of a single wavelength. Like in the case of phase masks, the feature sizes of the amplitude mask affect the spatial and spectral resolutions of imaging.[133] In the cases that involve lenses in addition to scattering masks, the average speckle size is equal to the diffraction-limited spot size; therefore, the lateral imaging resolution is given by $\sim\lambda/\mathrm{NA}$. In lensless cases such as LI-COACH and imaging systems with the pinhole array, the recording distances need to satisfy the far-field conditions to demonstrate the maximum resolution. Otherwise, a secondary bottleneck to imaging resolution is introduced.

3.3 Partial aperture imaging systems

Optical modulators are an integral part of the imaging systems. Manufacturing large-area optical modulators such as lenses and coded apertures is often challenging due to the enormous quantity of material involved, which leads to an increase in cost and weight. This is a common challenge faced when building telescopic systems. PAISs aim to image objects with a minimal area of the aperture without sacrificing the resolution. This approach minimizes the quantity of material and cost of imaging systems with large apertures such as telescopes. To understand the need for a partial aperture architecture, it is necessary to know the outcomes of different types of partial aperture configurations. A single diffractive lens-based imaging system is designed for the same simulation conditions as in the previous sections. The object distance has been set to infinity, and the image distance is set to 0.3 m. The imaging outcomes at the image plane for the USAF test object for different partial aperture imaging architectures are shown in Fig. 24. The images of circular, annular, semicircular, quadrant, and slit apertures are shown in Figs. 24(a)–24(e), respectively; magnified images of the PSFs are shown in Figs. 24(f)–24(j), respectively. The different types of distortions to images are noted for different architectures, as shown in Figs. 24(k)–24(o). Of all of the

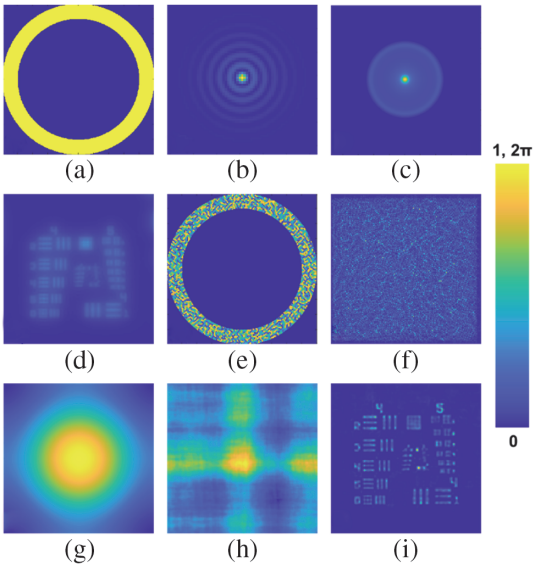

Figure 25 Image of (a) annular mask (50 pixels), (b) PSF, (c) MTF, and (d) direct imaging result of USAF object. (e) Phase image of the aperture of I-COACH, (f) PSH, (g) MTF, (h) OH, and (i) reconstruction result using nonlinear reconstruction for I-COACH.

results of direct imaging and I-COACH are shown in Fig. 26. With a decrease in the annulus width, the direct imaging result deteriorated while the results of I-COACH did not.

The phase mask for I-COACH was synthesized using GSA by adding an additional constraint of the annular aperture in the space domain. In this case, in addition to the nonlinear reconstruction, a technique of raising images to the power of p was applied.[140] The additional operation is a postprocessing method, so it does not affect the temporal resolution of imaging. The operation is expressed as $I_{R,p} = (I_R)^p$, which suppresses the background information when the matrix I_R is normalized. In the spectral domain, the above method can be expressed as a convolution, such that, for instance, when $p = l$, if G is the MTF corresponding to I_R, then $G_p = \mathcal{F}[\mathcal{F}^{-1}(G) \times \mathcal{F}^{-1}(G) \times \ldots l \text{ times}] = G * G * G \ldots l \text{ times}$. Therefore, with each increase in p, the bandwidth increases by the bandwidth of G. In the simulation results shown in Figs. 25 and 26, the value of p was 2.

4 Coherent Digital Holography

While having advantageous traits that enabled the previously surveyed holographic modalities, incoherent illumination cannot be used to explore phase-related phenomena. The disordered and random nature of the phase-fronts in spatially incoherent light makes it useless for phase imaging tasks that can profit from the task-designated engineered aperture. To align with this prospect, in the current chapter, we explore the path of COACH in the coherent regime and discuss possible applications and future opportunities.

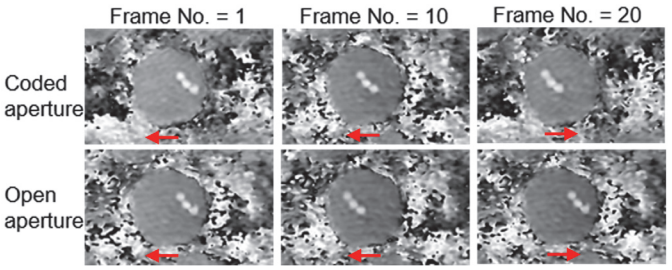

Figure 34 Selected frames from time-lapse videos of the reconstructed polystyrene microspheres' phases using COACH and conventional off-axis holography. Comparison between frames of the same serial number from each method emphasizes that reconstruction using coded aperture contains more temporal events. Red arrows signal the direction of the oscillating microspheres. Adapted from Ref. 156.

accumulates different background phases due to the different CPMs, the compensation effectively reveals the current event, whereas all of the others (one in this case) are destructed. Increased temporal resolution enabled by the COACH system compared with a standard MZI is further observed in Fig. 34, which illustrates selected shots from the final phase reconstruction video of the oscillating spherical structures using the two approaches. One can observe that the spheres' location in COACH lags compared with their location as they exit the conventional off-axis interferometer. The full time-lapse videos of both methods are available in the supplementary material of Ref. 156. Clearly, the demonstrated optical multiplexing approach using COACH can capture additional temporal information from the observed scene, which is otherwise lost, and effectively improves the system acquisition rate twofold. An interesting future research direction for this preliminary demonstration is to use a digital micromirror device as the CPM display device, since these devices are characterized by a much faster refresh time on the order of MHz,[157] which can significantly boost the temporal resolution.

To conclude this section, we have emphasized the advantageous possibilities opened when an external reference is introduced to the coherent COACH. Measuring the local phase delays across the probing wavefront becomes possible. In turn, the ability to modulate the wave's phase component with a predesigned diffractive optical element has stimulated the capabilities to increase the FOV and to speed the temporal events registered within a single hologram—two important aspects in optical microscopy.

4.3 Self-reference coherent digital holography

Unlike self-interference, the principle of self-reference has been known since the early days of holography, and its inventor Dennis Gabor used it when he recorded the first hologram in the late 1940s.[158] In essence, Gabor's first hologram was

to quantitative phase maps of transparent objects was successfully implemented.[56] Importantly, this phase-contrast-based phase retrieval (PCPR) method further stimulated the invention of the more-complete framework that will be surveyed in this section, the self-reference on-axis QPI (SO-QPI).[57] Phase pinhole[159] and PCPR[56] can be viewed as the enablers of SO-QPI since the former implements a simple phase-contrast microscope while the latter has treated the measured contrast map of the object as an on-axis hologram. The scalability of SO-QPI can be estimated from its derived implementations as a way to reduce the amount of data needed and increase the acquisition rate.[163,164] Another implementation based on the concept of self-reference was proposed with a light source having low spatial coherence, which reduces the out-of-focus noise in the reconstructed phase map.[165]

4.3.2 Self-reference on-axis quantitative phase imaging

SO-QPI combines the self-reference and the common-path features under a simple optical apparatus that provides motionless and accurate extraction of the phase information. This quantitative phase microscope relies on three different phase-contrast measurements of the same object. Considering the optical configuration shown in Fig. 35, the phase-contrast images in our system are formed by introducing a known phase delay of ξ radians between the zeroth-order and the higher-order components in the spatial spectral domain of the input object. The complex transmittance of the phase plate in Fig. 35 is implemented using an SLM. After inversely Fourier transforming the modified spatial spectrum, the emerging intensity pattern at the image plane reads as follows:

$$
\begin{aligned}
I(\bar{r};\xi) &= \left|\mathcal{F}^{-1}\left\{\mathcal{F}\left\{\exp\left[i\varphi\left(\frac{\bar{r}}{M_T}\right)\right]\right\}[1-\delta(\bar{\rho})+\delta(\bar{\rho})\exp(i\xi)]\right\}\right|^2 \\
&= \left|\mathcal{F}^{-1}\left\{\mathcal{F}\left\{1+\sum_{n=1}^{\infty}a_n\varphi^n\left(\frac{r}{M_T}\right)\right\}[1-\delta(\bar{\rho})+\delta(\bar{\rho})\exp(i\xi)]\right\}\right|^2 \\
&= \left|\mathcal{F}^{-1}\left\{\delta(\bar{\rho})+\mathcal{F}\left\{\sum_{n=1}^{\infty}a_n\varphi^n\left(\frac{r}{M_T}\right)\right\}[1-\delta(\bar{\rho})+\delta(\bar{\rho})\exp(i\xi)]\right\}\right|^2 \\
&= \left|\mathcal{F}^{-1}\left\{\delta^2(\bar{\rho})\exp(i\xi)+\mathcal{F}\left\{\sum_{n=1}^{\infty}a_n\varphi^n\left(\frac{\bar{r}}{M_T}\right)\right\}\right\}\right|^2 \\
&= \left|\exp(i\xi)+\sum_{n=1}^{\infty}a_n\varphi^n\left(\frac{\bar{r}}{M_T}\right)\right|^2 = 1+\exp(i\xi)\sum_{n=1}^{\infty}a_n^*\varphi^n\left(\frac{\bar{r}}{M_T}\right) \\
&\quad +\exp(-i\xi)\sum_{n=1}^{\infty}a_n\varphi^n\left(\frac{\bar{r}}{M_T}\right)+\left|\sum_{n=1}^{\infty}a_n\varphi^n\left(\frac{\bar{r}}{M_T}\right)\right|^2, \qquad (15)
\end{aligned}
$$

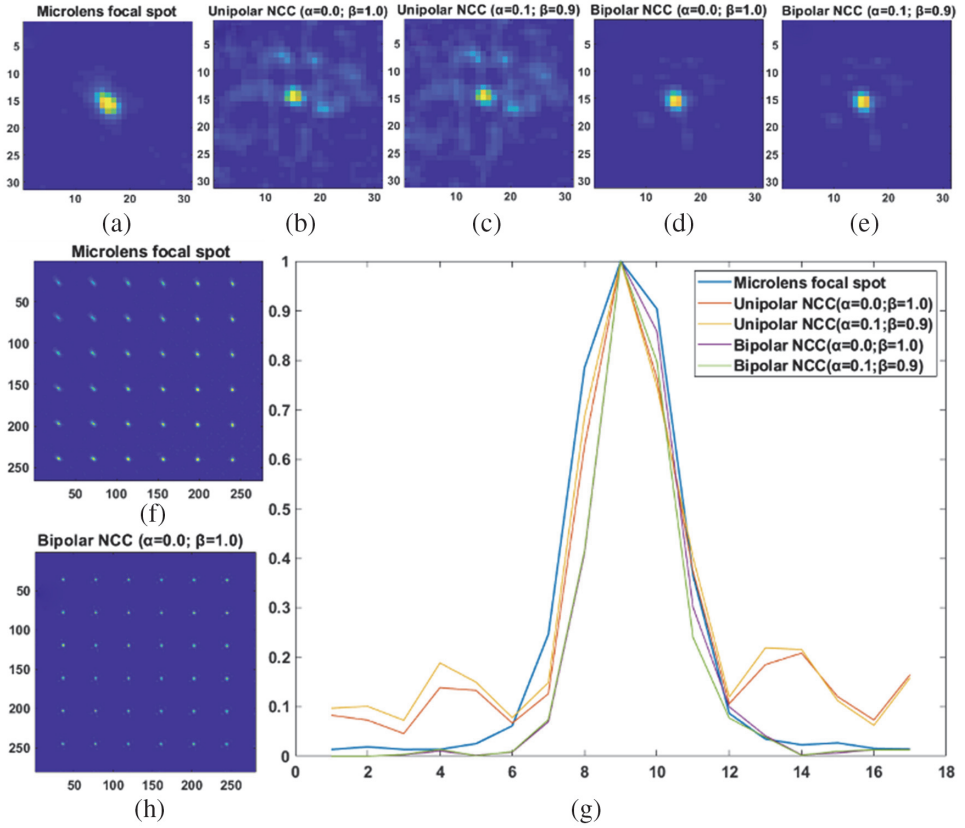

Figure 41 (a) Intensity response of a single microlens focal spot. Correlation peaks by unipolar NCC with (b) $\alpha = 0.0$, $\beta = 1.0$, (c) $\alpha = 0.1$, $\beta = 0.9$, and by bipolar NCC with (d) $\alpha = 0.0$, $\beta = 1.0$, (e) $\alpha = 0.1$, $\beta = 0.9$. (f) Intensity response of the microlens array for the test wavefront, (g) horizontal cross-section of the microlens focal spot and unipolar and bipolar correlation peaks. (h) Correlation peaks with bipolar NCC ($\alpha = 0.0$, $\beta = 1.0$) for the test wavefront. Adapted from Ref. 54.

unipolar COACH-based SHWS can offer approximately double the accuracy of the regular SHWS.

5 Summary and Conclusions

As we see in this Spotlight, the main topic of digital holography based on aperture engineering is divided into three main subareas. Two of them concentrate on incoherent digital holography, where one uses the effect of self-interference, and the other is interferenceless. The third subarea of digital holography with engineered apertures is devoted to coherent illumination. In general, the type of illumination dictates the applications for the different types of digital holography such that the incoherent systems are usually used for 2D and 3D intensity imaging. In

Joseph Rosen is the Benjamin Swig Professor of Optoelectronics with the School of Electrical and Computer Engineering, Ben-Gurion University of the Negev, Beer-Sheva, Israel. He has co-authored more than 300 publications. He is a Fellow of SPIE and Optica [formerly the Optical Society of America (OSA)]. His research interests include digital holography, optical microscopy, diffractive optics, statistical optics, biomedical optics, optical computing, and image processing.

Vijayakumar Anand is the ERA Chair and Associate Professor of Computational Imaging at the Institute of Physics, University of Tartu, Estonia. He is an adjunct Associate Professor at Optical Sciences Center, Swinburne University of Technology, Australia. He has co-authored more than 100 publications. He has been elected to the editorial board of Nature Springer's *Applied Physics B: Laser and Optics* and *Chinese Optics Letters*. His research interests include diffractive optics, digital holography and microfabrication.

Nathaniel Hai is a postdoctoral research fellow at the Wellman Center for Photomedicine, Boston, Massachusetts. His academic affiliations are with Massachusetts General Hospital and Harvard Medical School. He earned his bachelor's degree in physics and his doctorate in electrical engineering both from Ben-Gurion University of the Negev, Beer-Sheva, Israel. Nathaniel's research involves digital holographic microscopy and quantitative phase imaging to study pathology-related biomedical phenomena at the cellular and subcellular scale.